EUROPEAN ORGANIZATION FOR NUCLEAR RESEARCH

CERN/EP 82-110
21 July 1982

CHARGE CORRELATIONS IN DEEP INELASTIC PROTON-PROTON INTERACTIONS AT THE CERN ISR.

The Axial Field Spectrometer Collaboration

T. Åkesson[4], M.G. Albrow[6], S. Almehed[4], R. Batley[2], O. Benary[7], H. Bøggild[3], O. Botner[2], H. Brody[5], V. Burkert[2], A. Di Ciaccio[1], D. Cockerill[6], S. Dagan[7], E. Dahl-Jensen[3], I. Dahl-Jensen[3], G. Damgaard[3], C.W. Fabjan[2], S. Frankel[5], W. Frati[5], H. Gordon[1], A. Hallgren[2], K.H. Hansen[3], B. Heck[2], H.J. Hilke[2], J.E. Hooper[3], G. Jarlskog[4], P. Jeffreys[6], T. Jensen[2], G. Kesseler[2], T. Killian[1], D. Lissauer[7], B Lörstad[4], T. Ludlam[1], N.A. McCubbin[6], A. Melin[4], U. Mjörnmark[4], R. Møller[3], W. Molzon[5], B.S. Nielsen[2], A. Nilsson[4], L.H. Olsen[2], Y. Oren[7], L. Rosselet[2], E. Rosso[2], R.H. Schindler[2], B. Schistad[3], W.J. Willis[2], M. Winik[1], W. Witzeling[2], C. Woody[1]

[1] Brookhaven National Laboratory, USA
[2] CERN, Geneva, Switzerland
[3] Niels Bohr Institute, University of Copenhagen, Denmark
[4] University of Lund, Sweden
[5] University of Pennsylvania, USA
[6] Rutherford Appleton Laboratory, UK
[7] University of Tel-Aviv, Israel

Submitted to XXI International Conference on
High Energy Physics, Paris, 26-31 July 1982

ABSTRACT:

The production of charged particles in pp collisions at $\sqrt{s}$ = 63 GeV with an identified high p_T trigger particle emitted in the central region is studied. The measurements were performed at the CERN ISR using the Axial Field Spectrometer. The dependence of the ratio between positively and negatively charged particles on the identity, the transverse momentum and the rapidity of the trigger particle is investigated both in the system recoiling from the trigger particle and at small angles with respect to the trigger particle. The recoil system opposite to a positively charged trigger particle is nearly neutral, but shows a positive excess for negatively charged trigger particles. On the trigger side a charge compensating effect is seen, strongest for negatively charged trigger particles.

INTRODUCTION

We report on measurements of charged particles produced in pp collisions at $\sqrt{s}$ = 63 GeV with an identified high p_T charged particle emitted in the central region.

It is by now well established that in general such collisions give rise to a 4-jet structure [1,2]. (A more detailed investigation of the event structure seen in our data has been submitted to this conference). In the hemisphere containing the high p_T trigger particle other high p_T particles are closely collimated around the trigger particle direction. In the opposite hemisphere (the away side) high p_T particles are well collimated in azimuth opposite to the trigger direction, but form a broad enhancement in rapidity as the rapidity of the recoil jet varies from collision to collision.

A study of the quantum number correlations between the high p_T trigger particle and associated charged particles may help in distinguishing between different subprocesses on the parton level. An attempt in this direction has been made by the CDHW collaboration [1] which has presented detailed measurements of charge correlations in this type of interaction. Such measurements have also been published by the BFS collaboration [2].

The results presented here are preliminary. They are based on a subsample of our data and some acceptance corrections have yet to be made which are not expected to affect the conclusions presented below.

APPARATUS AND DATA ANALYSIS.

The experiment was performed at the CERN ISR using the Axial Field Spectrometer, shown in fig. 1 in a view transverse to the colliding beams. The apparatus and its performance are described in detail elsewhere [3]. Here we mention briefly only those components of the apparatus which were used in the present investigation.

The central cylindrical drift chamber is 1.4 m long and extends radially from 0.2 to 0.8 m. It is segmented azimuthally in 4° sectors each with 42 sense wires. In azimuth it provides a full 2π coverage except for two 16° wedges above and below the interaction region. It is situated in an axially symmetric magnetic field of ~ 0.5 T.

Three sets of threshold Cerenkov counters subtend an azimuthal angle of 45° and $45^{\circ} < \theta < 135^{\circ}$ in polar angle. The aerogel Cerenkov counter was not used in the present analysis. The high pressure and the atmospheric pressure counters are subdivided into 12 and 18 optical cells, respectively. The average number of photoelectrons produced by a $\beta \simeq 1$ particle is ~ 20 in the high pressure counter and ~ 10 in the atmospheric pressure counter. The two sets of counters allow pion/heavy particle discrimination for $p > 2$ GeV/c and provide pion, kaon and proton separation for $p > 6$ GeV/c.

Two sets of proportional wire chambers cover the same solid angle as the Cerenkov counters. Their use is described below.

Copper calorimeters placed behind the atmospheric pressure counters cover $\sim 1/7$ of the solid angle of these counters. They were installed to provide a cross-check of the momentum measurement at $p > 8$ GeV/c and were also used in the trigger for about half the data sample.

Interactions resulting in the production of a high p_T charged particle within the solid angle of the Cerenkov counters were selected using a three level trigger. The first level uses a scintillator hodoscope surrounding the beam pipe together with groups of wires in the PWC's to require $p_T > 0.8$ GeV/c. The second level uses individual wire hits in the PWC's and the last level uses a microprocessor operating on the appropriate drift chamber signals. For details see ref. [4].

The data were collected in September and December 1981 and in March 1982. They were first passed through the AFS drift chamber reconstruction and fitting programs [5]. Events were accepted if they contained a reconstructed primary vertex, a condition fulfilled by 99% of the events.

Cuts were imposed on the tracks to ensure that they belonged to the event and that their momenta were reasonably well determined ($\Delta p/p < 0.06$ for $p < 2$ GeV/c and $\Delta (1/p) < 0.03$ for $p > 2$ GeV/c). All tracks were tranformed to the c.m.s., using a pion mass except for identified trigger particles. From a study of 'minimum bias' events and comparisons with earlier inclusive measurements it was found that with the above mentioned cuts the acceptance is nearly uniform in rapidity for $|y| < 0.8$ and uniform in azimuth for $|\phi| < 80^{\circ}$ and $110^{\circ} < \phi < 250^{\circ}$ (with $\phi = 0$ along an axis through the middle of the Cerenkov counters). The p_T spectra agreed well with earlier data both in normalization and shape for 0.2 GeV/c $< p_T <$ 5 GeV/c. For the data presented here the interaction region was larger and the acceptance in rapidity is uniform for $|y| < 0.6$ only, but is still larger than 50% at a rapidity of $\pm$ 0.8. Cuts on associated particles were made in rapidity of $\pm$ 0.8 and in p_T of 5 GeV/c . No corrections have been applied for the gaps up and down or for the reduced acceptance for $|y| > 0.6$. Also no corrections were made for a reduced efficiency for tracks crossing the trigger track. The loss was found to be $\sim$ 15% inside an angle of 10° to the trigger track assuming that the number of close crossing and non-crossing tracks are the same. Data were collected with both signs of the magnetic field. The ratio of the charge ratios measured with different magnet polarity was 1.010 $\pm$ 0.014 overall. The ratio was also calculated in many regions of phase space, where the charge ratios themselves differed considerably from unity. No significant differences were found for different magnet polarities.

Tracks within the acceptance of the Cerenkov counters, in particular the high p_T trigger tracks, were passed through another set of programs. Their momenta were refitted using both the drift chamber information and the reconstructed space points in the PWC's. This procedure served to reject simulated high p_T tracks from the drift chamber (e.g. due to very flat decays), to reject particles interacting in the material of the Cerenkov counters, and to improve the momentum resolution to approximately $\Delta p/p \sim 10\%$ at $p = 10$ GeV/c. The procedure was tested using high momentum cosmic ray muons where the momentum was measured over both half-cylinders of the drift chamber.

The signals from the Cerenkov counters were then used to identify particles with sufficiently high momenta. After appropriate cuts (on the distance to mirror edges or to PM's) the identified heavy particle samples are estimated to be very clean whereas the pion sample may be contaminated by heavier particles on the few percent level, mainly due to γ-conversions from an overlapping π^0 decay.

The present sample contains 25,000 events with an identified trigger particle with $p_T > 3$ GeV/c (10,000 with $p_T > 4$ GeV/c). The rapidity of the trigger particle is distributed with $|y| < 0.225$ for 16,000 events, $|y|$ between 0.225 and .45 for 5,000 events and $|y|$ between 0.45 and 1 for 4,000 events. The lowest rapidity interval includes the events taken with the copper calorimeters included in the trigger

RESULTS

We shall treat the trigger jet and the away side jet separately. For charge correlations in the trigger jet we shall use the variable Z_F defined for an associated particle as the ratio between its momentum along the trigger direction and the momentum of the trigger particle, i.e $Z_F = (\vec{p}^{as} \cdot \vec{p}^{trig}/|p^{trig}|^2$. Fig. 2 shows for associated particles with $Z_F > 0.25$ the distribution in cosine of the angle, ψ, between the trigger direction and the associated particle direction. The distribution is shown for π triggers with $|y| < 0.225$ and for three intervals of trigger p_T. With increasing trigger p_T the distribution becomes narrower as one would expect if the transverse momenta of associated particles are limited with respect to the trigger momentum. Fig. 3 shows for $\psi < 40^o$ the distribution $(1/N_{trig})\ dN_{as}/dZ_F$ as a function of Z_F, again for π triggers in the central rapidity interval and for three trigger p_T intervals. The distribution becomes steeper with increasing p_T.

In fig. 4 we show the ratio between the number of particles with the same charge as the trigger particle and the number of particles with charge opposite to that of the trigger particle as a function of Z_F and for $\psi < 40^o$ and trigger rapidity $|y| < 0.225$. For all types of trigger particles, π^+, π^- and h^- ($h^- = K^-$ or $\bar{p}$) a charge compensating effect is seen which increases with Z_F. The effect seems rather independent of trigger p_T but is stronger for π^- than for π^+ triggers and possibly stronger still for h^- triggers. This charge compensating effect is strongest in the azimuthal region around the trigger, but extends over a broad range in azimuth. This is shown in fig. 5, where the ratio between positively and negatively charged associated particles is given as a function of the difference in azimuthal angle between the trigger particle and the associated particles.

We next discuss the away side jet. Here we shall use the variable X_E defined as $X_E = -(\vec{p}_T^{trig} \cdot \vec{p}_T^{as})/|p_T^{trig}|^2$. The distribution $(1/N_{trig})\, dN_{as}/dX_E$ is shown in fig. 6 as a function of X_E for three intervals of trigger p_T, again for π triggers with $|y| < 0.225$. This distribution is more independent of trigger p_T than the corresponding distribution in Z_F. The charge ratios as a function of X_E are, within our statistics, independent of the trigger p_T over our p_T-range from 3-8 GeV/c. We show in fig. 7 the charge ratios as a function of X_E for all trigger rapidities and for trigger p_T between 3 and 8 GeV/c. The ratio between positively and negatively charged associated particles is nearly independent of X_E and close to 1 for π^+ and for h^+ triggers. For π^- and h^- triggers the ratio increases with X_E from a value close to 1 to a value around 1.5 to 2.

Finally we show in fig. 8 the dependence of the charge correlations on the rapidity of the trigger particle. Fig. 8a) shows the charge compensating effect on the trigger side for π triggers and for the Z_F interval from 0.2 to 0.6 in three intervals of trigger rapidity (for the outer rapidity intervals only the associated particles inside the half cone away from the beams have been counted). The data are clearly consistent

with no dependence of the charge compensating effect on rapidity but a charge compensation increasing gently with trigger rapidity is not excluded. Fig. 8b) shows the away side charge ratio for the X_E interval from 0.2 to 0.6, again for π triggers and for three intervals of trigger rapidity. The data are consistent with a charge ratio independent of trigger rapidity.

ACKNOWLEDGEMENTS

We acknowledge with thanks the work of the CERN EP, EF and ISR devisions on the construction and installation of the Axial Field Spectrometer, and the contributions to the experiment of P. Dam, W.M. Evans, P. Frandsen, M.D. Gibson, J.W. Hiddleston, H. Hofmann, J. v.d. Lans, J. Lindsay, E. Lohse and A. Rudge. Support from the Research Councils in our home countries is gratefully acknowledged.

REFERENCES

[1] a) W. Geist, rapp. talk Kazimierz Symposium 1981.
b) H.G. Fisher, rapp. talk, EPS Conf. High Energy Physics, Lisbon 1981.
c) P. Hanke, Rencontre de Moriond 1982.

[2] M.G. Albrow et al., Nuclear Physics B145 , (1978) 305.

[3] a) H. Gordon et al., Nucl. Inst. & Methods 196 (1982) 303.
b) O. Botner et al., Nucl. Instr. Methods 196 (1982) 315.

[4] B. Heck et al., EPS Conf. on Computing, Bologna 1980.

[5] S. Almehed and B. Lörstad, Comput. Phys. Comm. 22, 1981.

FIGURE CAPTIONS

Fig. 1. The Axial Field Spectrometer (view transverse to the collision axis). The magnet coils are in fact out of the plane, on the poles. The left calorimeter wall is shown in a retracted position.

Fig. 2. The distribution of associated particles as a function of cosine of the angle, ψ, between the trigger momentum and the associated particle momentum, for associated particles with $Z_F > 0.25$ (see text for definition of Z_F) and for π triggers with rapidity $|y| < 0.225$. The distribution is shown for three intervals of trigger p_T.

Fig. 3. The distribution $(1/N_{trig})(dN_{as}/dZ_F)$ as a function of Z_F (on the trigger side, with $\psi < 40^o$).

Fig. 4. The ratio between the numbers of associated particles with the same charge and the opposite charge to that of the trigger particles. The ratio is shown for π^+, π^- and h^- (i.e. K^- and $\bar{p}$) triggers and for the two p_T^{trig} intervals 3-4 GeV/c and 4-8 GeV/c.

Fig. 5. The ratio between the numbers of positively and negatively charged associated particles with $p_T > 0.5$ GeV/c as a function of the difference in azimuthal angle between the trigger particle direction and the associated particle direction.

Fig. 6. The distribution $(1/N_{trig})(dN_{as}/dX_E)$ as a function of X_E. (on the away side, see text for definition of X_E).

Fig. 7. The +/- charge ratio as a function of X_E for different trigger particle types.

Fig. 8. a) The same ratio as in fig. 4 as a function of trigger particle rapidity. The ratio is shown for π triggers and for the Z_F interval from 0.2 to 0.6.(Trigger side).
b) The +/- charge ratio as a function of trigger rapidity. The ratio is shown for π triggers and for the X_E interval from 0.2 to 0.6.(Away side).

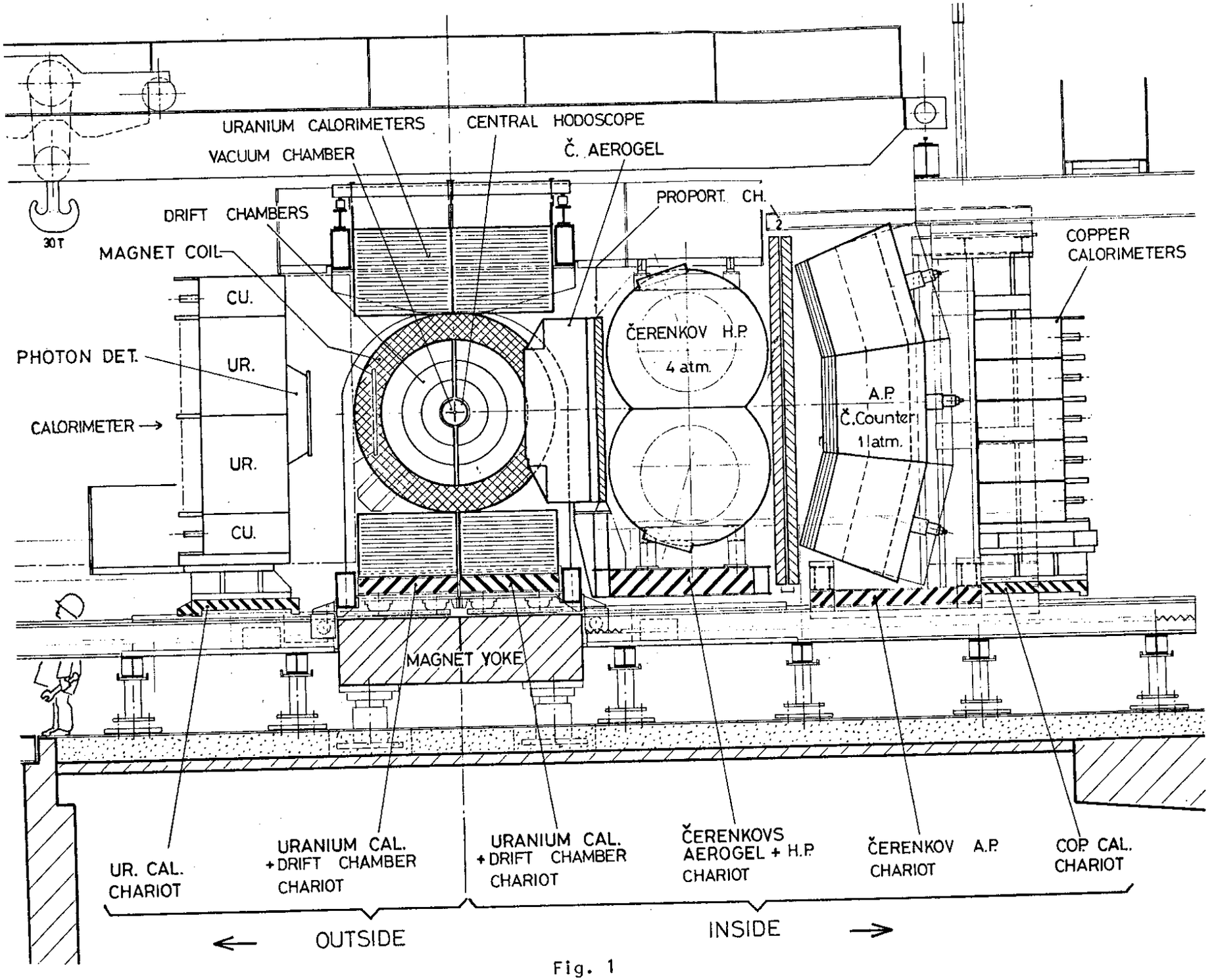
URANIUM CALORIMETERS
CENTRAL HODOSCOPE
VACUUM CHAMBER
Č. AEROGEL
PROPORT. CH.
DRIFT CHAMBERS
30T
MAGNET COIL
COPPER CALORIMETERS
CU.
PHOTON DET.
UR.
ČERENKOV H.P.
4 atm.
CALORIMETER →
A.P.
Č.Counter
1 atm.
UR.
CU.
MAGNET YOKE
UR. CAL. CHARIOT
URANIUM CAL. + DRIFT CHAMBER CHARIOT
URANIUM CAL. + DRIFT CHAMBER CHARIOT
ČERENKOVS AEROGEL + H.P. CHARIOT
ČERENKOV A.P. CHARIOT
COP. CAL. CHARIOT
← OUTSIDE
INSIDE →

Fig. 1

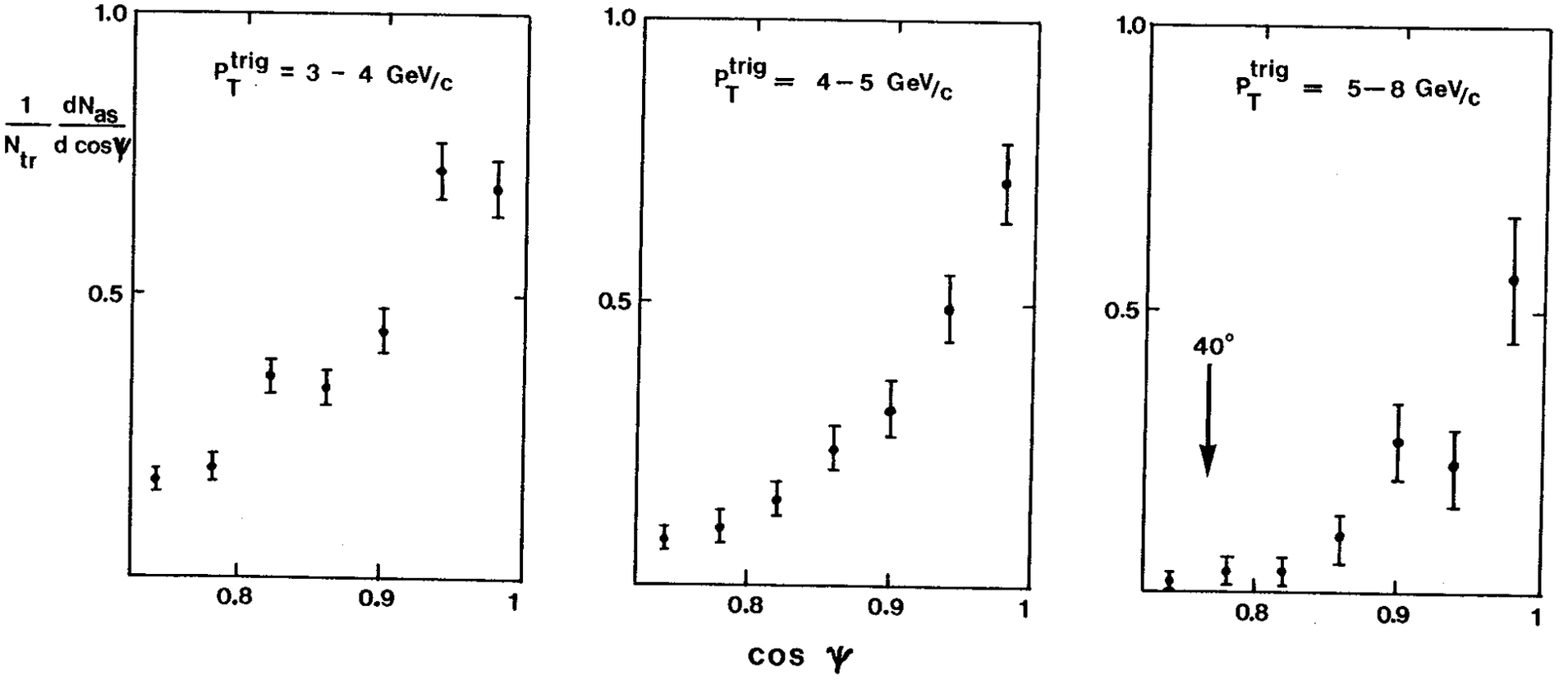
π-Triggers , $|y^{trig}| < 0.225$, $z_F > 0.25$
$\frac{1}{N_{tr}} \frac{dN_{as}}{d\cos\psi}$
p_T^{trig} = 3 - 4 GeV/c
p_T^{trig} = 4 - 5 GeV/c
p_T^{trig} = 5 - 8 GeV/c
40°
1.0
0.5
0.8
0.9
1
cos ψ

Fig. 2

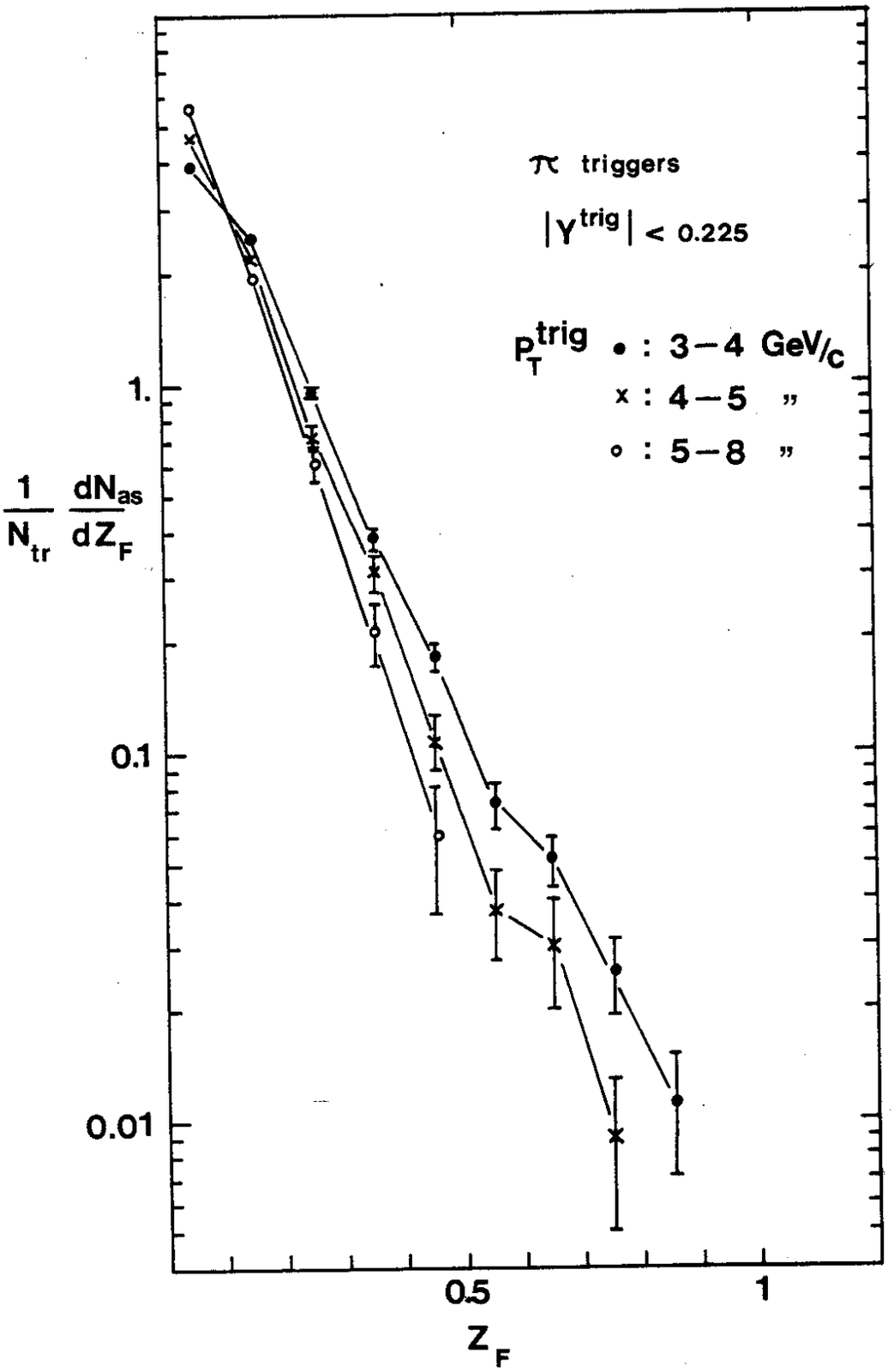
π triggers
|Y^trig| < 0.225
P_T^trig • : 3−4 GeV/c
x : 4−5 "
∘ : 5−8 "
1.
0.1
0.01
1/N_tr dN_as/dZ_F
0.5
1
Z_F

Fig. 3

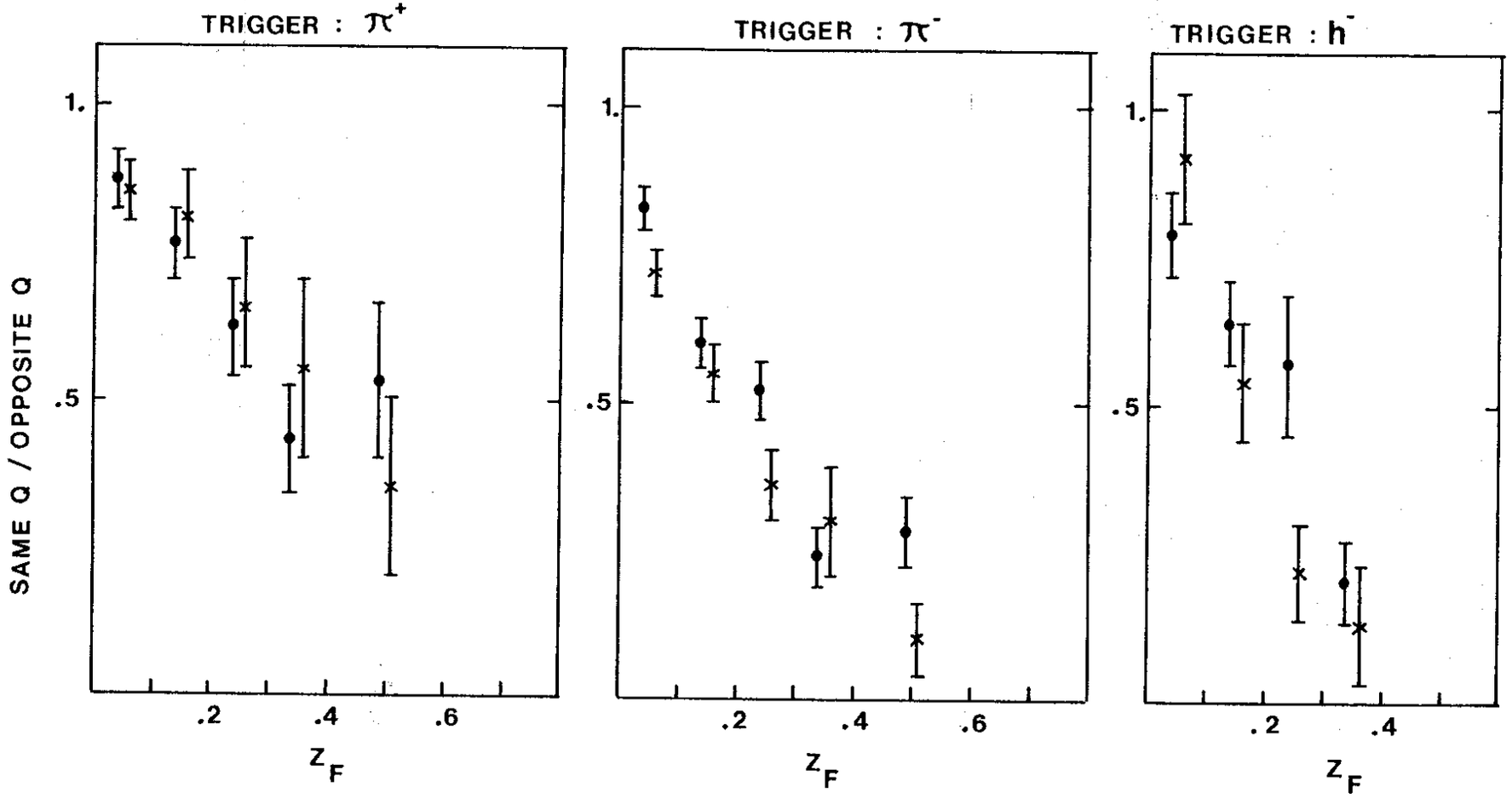
$|Y^{trig}| < 0.225$
P_T^{trig} : • 3−4 GeV/c
x 4−8 ,,
TRIGGER : π^+
TRIGGER : π^-
TRIGGER : h^-
SAME Q / OPPOSITE Q
1.
.5
.2
.4
.6
Z_F

Fig. 4

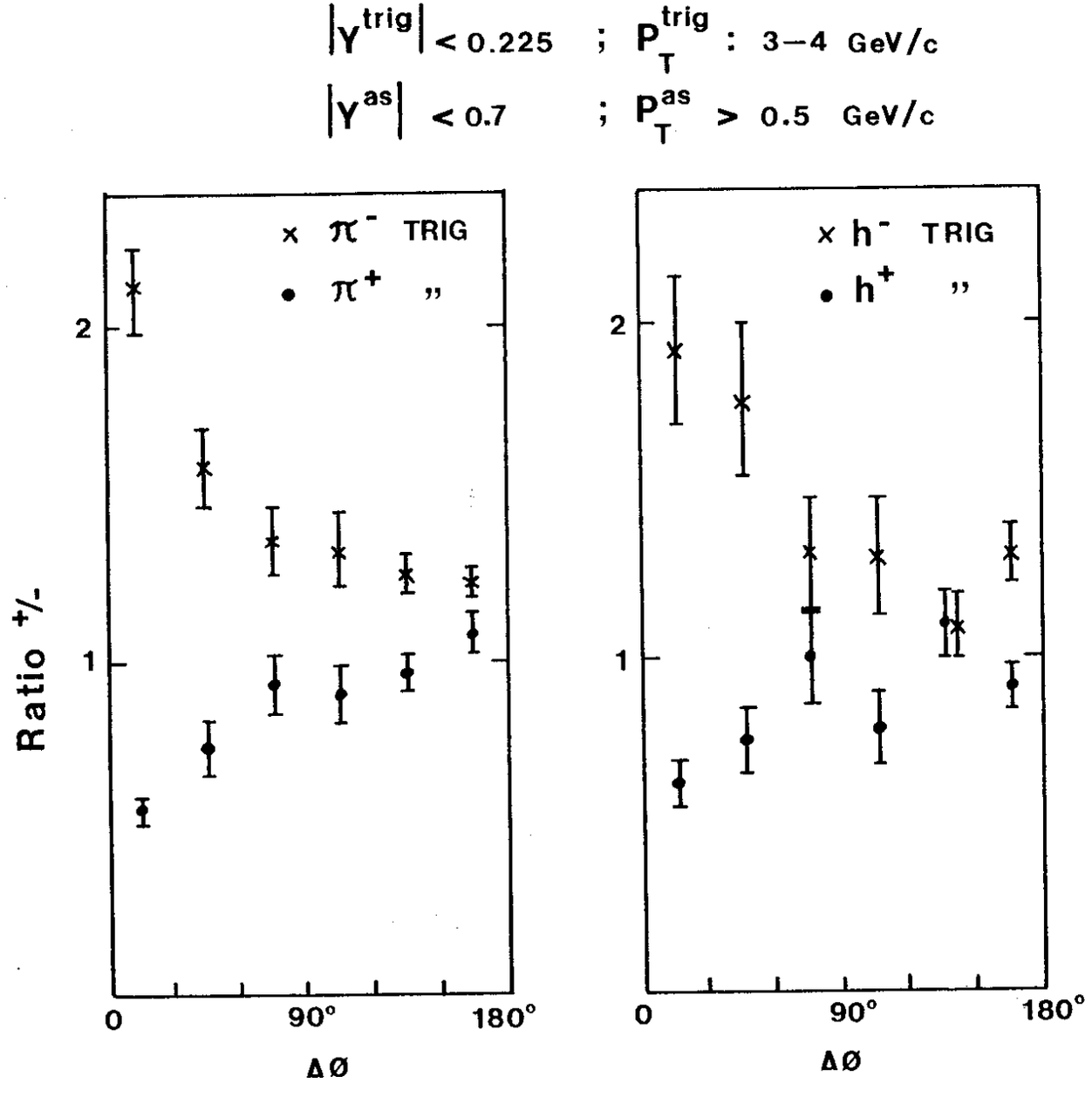
$|Y^{trig}| < 0.225$; P_T^{trig} : 3–4 GeV/c
$|Y^{as}| < 0.7$; $P_T^{as} > 0.5$ GeV/c
× π⁻ TRIG
• π⁺ ”
× h⁻ TRIG
• h⁺ ”
Ratio +/-
2
1
0
90°
180°
ΔØ

Fig. 5

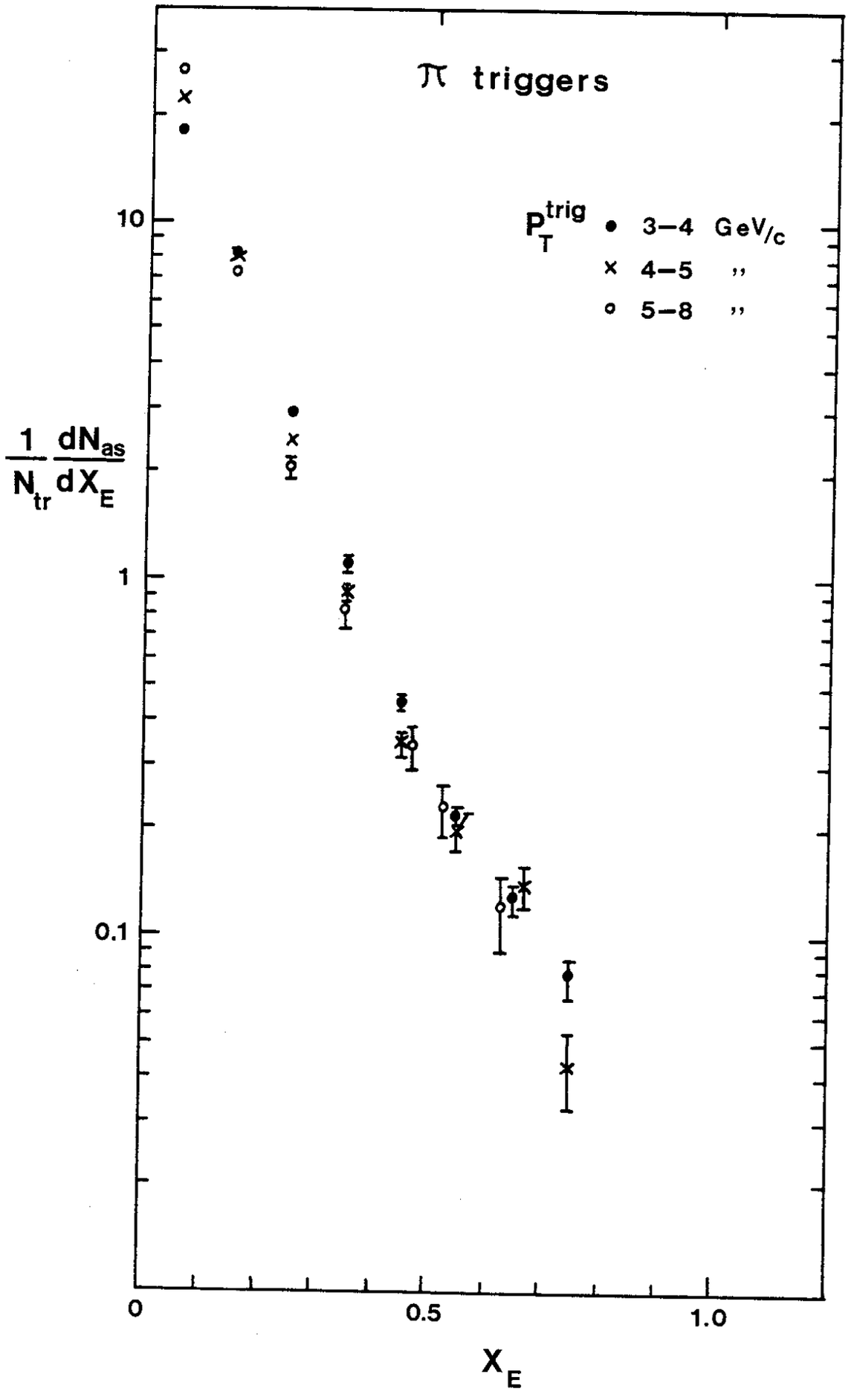
π triggers
P_T^{trig}
• 3–4 GeV/c
× 4–5 ,,
○ 5–8 ,,
$\frac{1}{N_{tr}} \frac{dN_{as}}{dX_E}$
10
1
0.1
0
0.5
1.0
X_E

Fig. 6

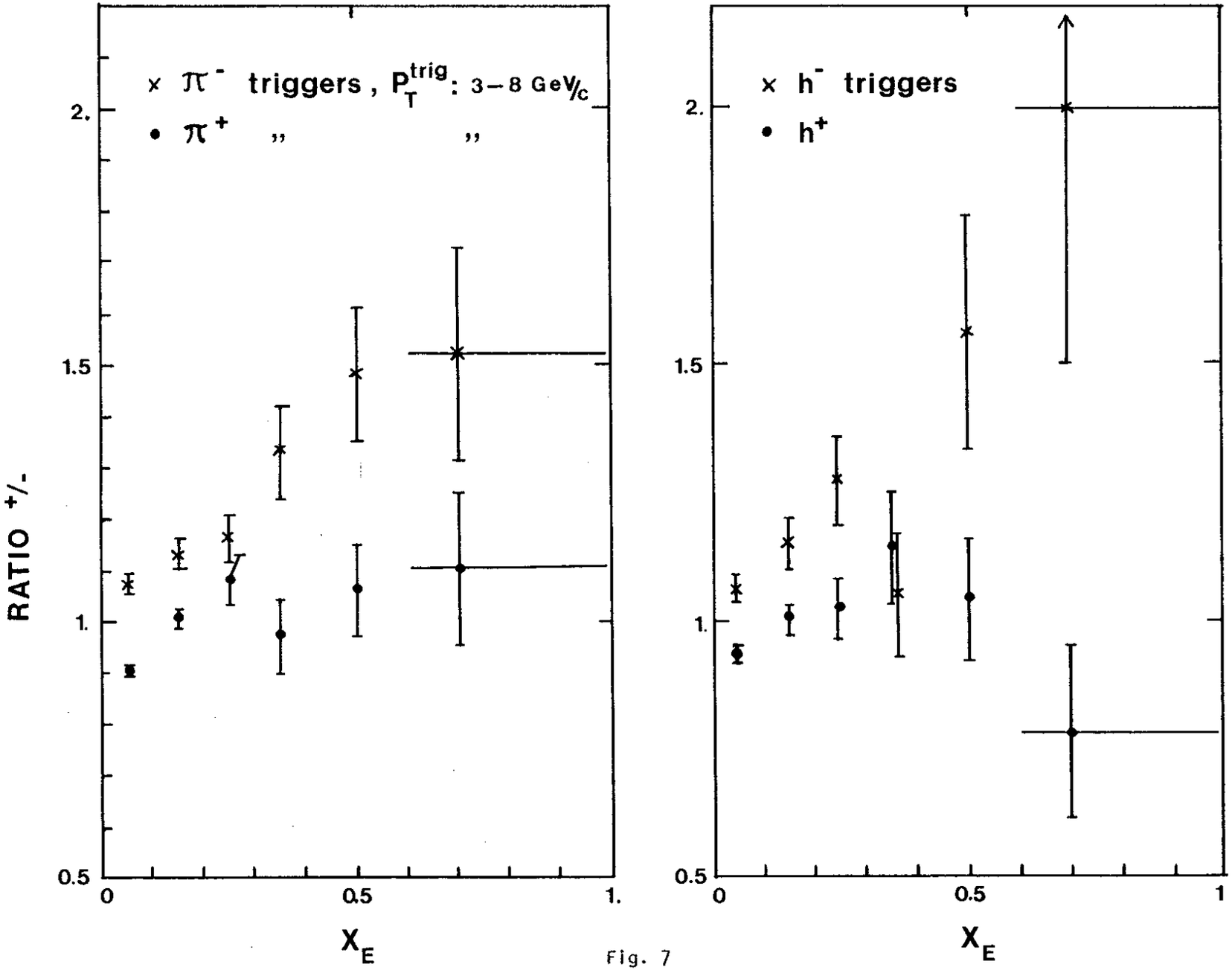
× π⁻ triggers, P_T^trig: 3–8 GeV/c
• π⁺ „ „
× h⁻ triggers
• h⁺
RATIO +/-
X_E
X_E
2.
1.5
1.
0.5
0
0.5
1.

Fig. 7

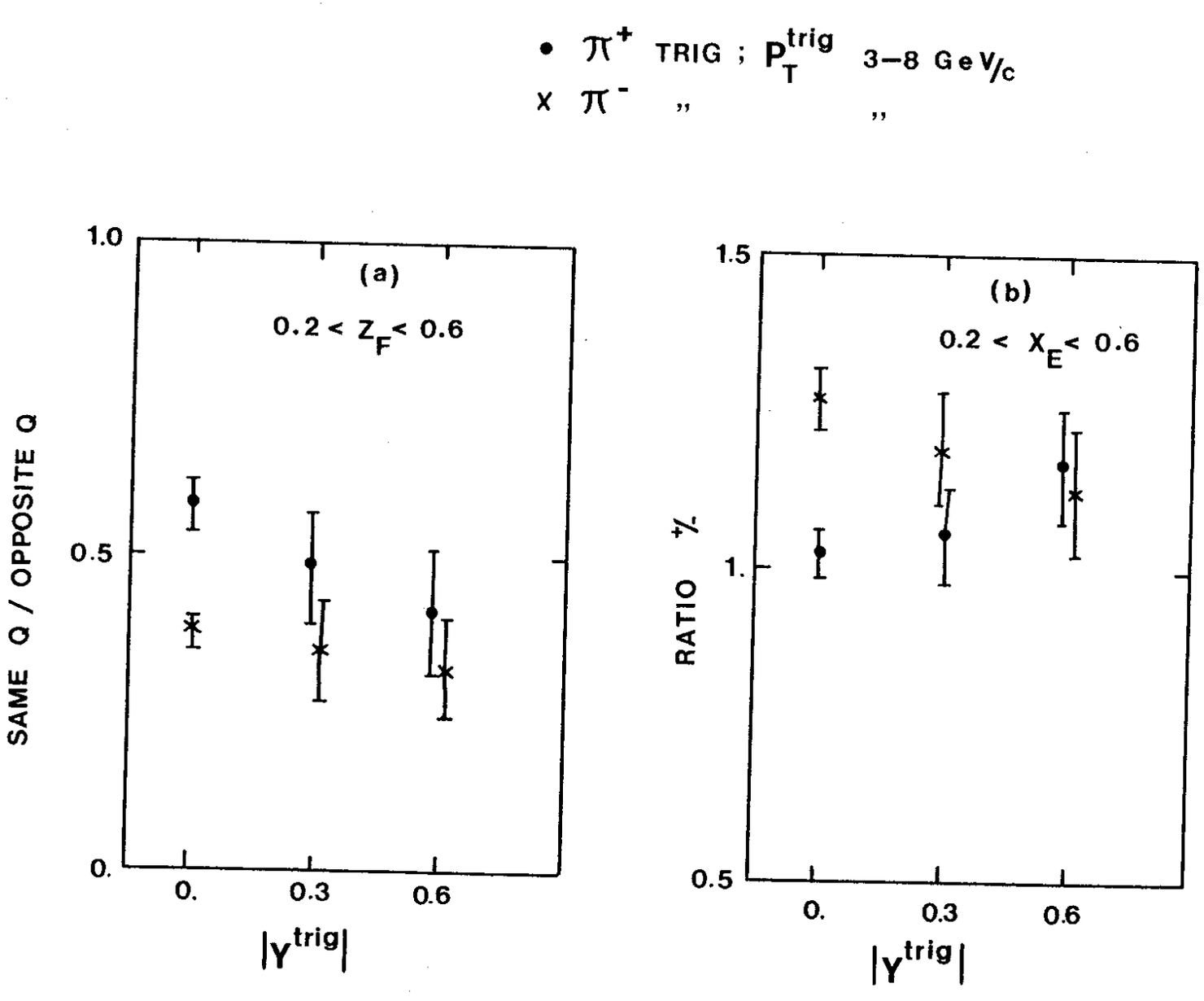
• π+ TRIG ; P_T^trig 3–8 GeV/c
x π- „ „
(a)
0.2 < Z_F < 0.6
SAME Q / OPPOSITE Q
1.0
0.5
0.
0.
0.3
0.6
|Y^trig|
(b)
0.2 < X_E < 0.6
RATIO +/-
1.5
1.
0.5
0.
0.3
0.6
|Y^trig|

Fig. 8a

Fig. 8b